

# Reformulation of the MODTRAN band model for higher spectral resolution

Alexander Berk<sup>\*a</sup>, Prabhat K. Acharya<sup>a</sup>, and Lawrence S. Bernstein<sup>a</sup>  
Gail P. Anderson<sup>b</sup>, James H. Chetwynd<sup>b</sup>, and Michael L. Hoke<sup>b</sup>

<sup>a</sup> Spectral Sciences, Inc., 99 S. Bedford St., Burlington, MA 01803

<sup>b</sup> USAF Research Laboratory, Space Vehicles Directorate Hanscom AFB, MA 01730

## ABSTRACT

The MODTRAN 1 cm<sup>-1</sup> band model has been reformulated for application to higher spectral resolution. Molecular line center absorption is still determined from finite spectral bin equivalent widths but is now partitioned between the bin containing the molecular transition and its nearest neighbor bin. Also, the equivalent width calculation has been upgraded to retain to maintain high accuracy at the increased spectral resolution. The MODTRAN Lorentz line tail spectral bin absorption coefficient data has been replaced by a more general and accurate Padé approximant for Voigt line tails, and higher order pressure dependencies are now modeled. Initial comparisons to the FASE model and to measurement data are presented.

**Keywords:** MODTRAN, remote sensing, hyperspectral, imaging, band model, infrared, radiative transfer, molecular transmittance

## 1. INTRODUCTION

MODTRAN4<sup>1,2</sup> is the U.S. Air Force (USAF) standard moderate spectral resolution radiative transport model for wavelengths extending from the thermal InfraRed (IR) through the visible and into the ultraviolet (0.2 to 10,000.0 μm). The MODTRAN4 1 cm<sup>-1</sup> statistical band model was developed collaboratively by Spectral Sciences, Inc. and the USAF Research Laboratory, and it provides a fast alternative (100-fold increase in speed) to the USAF first principles and more accurate line-by-line (LBL) radiative transport models, FASCOD<sup>3</sup> and FASCOD for the Environment, FASE<sup>4</sup>. Comparisons between MODTRAN4 and FASE spectral transmittances and radiances show agreement to within a few percent or better in the thermal IR. MODTRAN4 includes flux and atmosphere-scattered solar calculations, essential components in analysis of near-IR and visible spectral region data that are not readily generated by LBL models.

MODTRAN4 and its predecessors have been used extensively over the last quarter century in the design and analysis of broadband, multiband, and short-wave IR / Visible hyperspectral imaging sensors. However, conventional interferometers and many state-of-the-art and next-generation hyper- and ultra-spectral imaging sensors working in the long- and mid-wave IR will operate at higher spectral resolution than MODTRAN4 provides. In parallel with this instrument evolution, SERTRAN, a Spectrally Enhanced Resolution version of MODTRAN, has been developed. SERTRAN retains all MODTRAN4 capabilities while providing a factor of 10 improvement in spectral resolution. Key MODTRAN4 features adopted by SERTRAN include stratified molecular and aerosol atmospheres, Bi-directional Reflectance Distribution Function (BRDF) ground surfaces with adjacency effect modeling, spherical refractive geometry, a statistical Correlated-*k* (CK) algorithm<sup>5</sup> and solar and thermal scattering from multiple stream models. Due to its higher spectral resolution, SERTRAN also improves treatment of line correlation and increases overall accuracy when compared to MODTRAN4 and runs up to a factor of 10 slower than MODTRAN4, but still considerably faster than LBL radiative transport models.

Narrowing the band model spectral resolution changes the fundamental character of the band model. The half-width of molecular transitions near sea level average about 0.07 cm<sup>-1</sup>, which is comparable to the SERTRAN spectral bin width. As illustrated in Figure 1, the 1.0 cm<sup>-1</sup> band model calculates the absorption of molecular lines whose line center regions lie almost entirely within the spectral bin. At the higher spectral resolution, a much larger fraction of each molecular line falls outside of the spectral bin containing the line. Reformulation of the MODTRAN4 band model for SERTRAN has therefore

---

\* Correspondence: Email: lex@spectral.com, www.spectral.com; Telephone 781 273-4770; Fax: 781 270-1161

required improved treatment of both line tail and line center absorption. Line tail absorption is modeled nearer line centers, and the finite-bin single-line equivalent width used to calculate line center absorption is no longer simply a small perturbation of the total single line equivalent width. In this paper, the differences between the MODTRAN4 and SERTRAN band models are described. Model results for the IR are validated by comparison to LBL models and high spectral resolution measurement data.

## 2. THE SERTRAN BAND MODEL

While this paper highlights differences between the MODTRAN4 and SERTRAN band models, it is important to note that the two models do share major radiative transport elements. The basic quantities computed by the band models are individual species spectral transmittances through homogeneous path segments. These segments are defined within single atmospheric layers if the CK algorithm is selected and for Curtis-Godson<sup>6,7</sup> averaged paths otherwise. The individual species transmittances are themselves computed as a product of three terms: the molecular continuum ( $\Delta\nu > 25.5 \text{ cm}^{-1}$ ), line tails and line centers. Only the line tail and line center calculations differ between MODTRAN4 and SERTRAN. MODTRAN4 and SERTRAN use the same  $\text{H}_2\text{O}$  and  $\text{CO}_2$  continua as FASE. Molecule-to-molecule line overlap is presumed to be uncorrelated so the combined species transmittance is the product of the individual values.

Once the combined transmittances are computed, the spectral radiance and flux calculations in MODTRAN4 and SERTRAN proceed in identical fashion. A linear-in-tau algorithm models the variation in the thermal emission across atmospheric layers. This calculation requires layer molecular absorption optical depths, which are computed from the transmittances. The thermal calculation also requires aerosol, cloud and Rayleigh optical depths; these are derived from default or user-defined optical and profile data. The single and multiple scattering radiance calculations also depend on default or user-defined scattering phase functions and on single scattering albedo profiles; the scattering albedos are computed from the optical depth data. All these values are used to calculate single-scatter solar radiance and are also input to either a simple 2-stream multiple scattering model<sup>8</sup> or to the DISORT<sup>9</sup> N-stream discrete ordinate routine. The outputs from the scattering models are the thermal and solar multiple scattering path radiance contributions and level flux values.

### 2.1 SERTRAN band model line center absorption

The line center absorption within a spectral bin is generally defined as the in-band absorption from all molecular transitions centered in that bin, Figure 2. LBL models calculate this in-band absorption by explicitly determining the spectral absorption of each line on a fine spectral grid and then integrating the resulting spectrum. In a band model approach, the in-band absorption is approximated based on statistical assumptions regarding line positions and overlap. Temperature dependent band model parameters are computed from a molecular transition line atlas such as HITRAN<sup>10</sup>. These parameters define an effective single-line absorption line strength for the interval and the effective number of lines,  $n_{eff}$ .

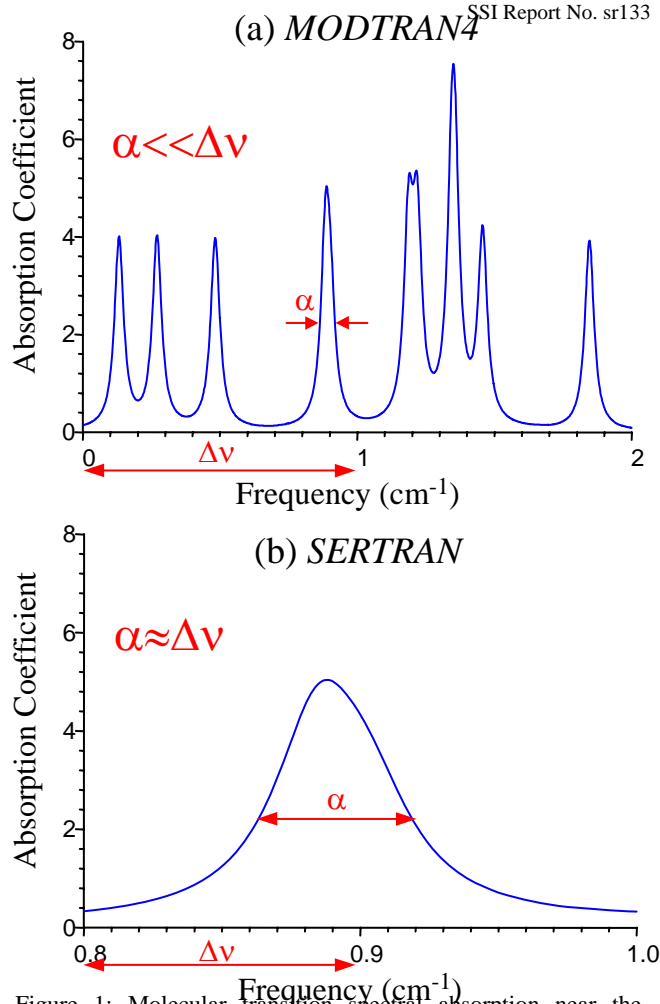


Figure 1: Molecular transition spectral absorption near the ground: (a) Spectral features within a MODTRAN 1.0  $\text{cm}^{-1}$  bin; (b) Spectral features within a SERTRAN 0.1  $\text{cm}^{-1}$  bin.

In MODTRAN4, the finite spectral bin single-line Voigt equivalent width  $W_{sl}$  is computed to determine the absorption of the effective average line. It is calculated as the difference between the total equivalent width - computed using the Rodgers-Williams formula<sup>11</sup> and the absorption due to the line tails falling outside of the spectral band. The line tail calculations are performed for a line centered  $0.2 \text{ cm}^{-1}$  from the edge of the  $1.0 \text{ cm}^{-1}$  spectral bin; offsetting the location of the effective line from the center of the bin gives a more representative result for the average contribution of the line tails. MODTRAN4 computes the line tail absorption by modeling the tail line-shape as being inversely proportional to the square of the line center displacement, i.e.,  $\propto (\Delta\nu)^{-2}$ . With lines centered  $0.2 \text{ cm}^{-1}$  from the edge of the spectral band, Doppler contributions to the line tails are small and the Lorentz line-shape denominator is dominated by the line center displacement term for Lorentz half-widths less than  $0.1 \text{ cm}^{-1}$ .

MODTRAN4 computes the total  $1.0 \text{ cm}^{-1}$  spectral band transmittance  $T_\nu$  for the  $n_{eff}$  identical lines by assuming line overlap characteristic of randomly distributed lines within a spectral interval. Plass<sup>12</sup> showed that the transmittance due to randomly distributed identical lines is given by the expression

$$T_\nu = \left(1 - \frac{W_{sl}}{\Delta\nu}\right)^{n_{eff}} \quad (1)$$

The Plass transmittance reduces to exact expressions in the limit of a single line,  $T_\nu(n_{eff} = 1) = 1 - W_{sl}/\Delta\nu$ , and in the many line limit,  $T_\nu(n_{eff} \rightarrow \infty) = \exp(-n_{eff} W_{sl}/\Delta\nu)$ .

At the higher spectral resolution of SERTRAN, direct application of the MODTRAN4 band model is computationally difficult. For instance, with a  $\Delta\nu = 0.1 \text{ cm}^{-1}$  spectral bandwidth and an effective average line positioned  $0.2 \Delta\nu$  from the bin edge, line tail absorption contains significant Voigt contributions. In SERTRAN, the displacement of line tails from line center is increased from  $0.02 \text{ cm}^{-1}$  to  $0.1 \text{ cm}^{-1}$  by modifying the band model partitioning of line center and tail absorption. SERTRAN defines the band model line center absorption as the in-band absorption from all lines centered in the selected bin *and all lines centered within half a bandwidth of the selected bin*. With this definition, the line center absorption of each molecular transition is partitioned between 2 spectral bins. On average, half the lines contributing to the interval are centered in the interval and half are centered outside the interval. Thus, the finite-bin equivalent width is computed for a line centered precisely on the edge of the spectral bin. The total in-band absorption from the edge-centered line is therefore one-half the difference between the total equivalent width of the line and the  $0.1 \text{ cm}^{-1}$  tail.

Since atmospheric molecular line half-widths can be as large as  $0.13 \text{ cm}^{-1}$ , the  $0.1 \text{ cm}^{-1}$  line tails cannot be modeled as simply being inversely proportional to the square of the line center displacement. The finite-bin equivalent width calculations were upgraded for SERTRAN, and the details of the upgraded algorithms will be presented in a subsequent paper. Figure 3 summarizes the results. The MODTRAN4 calculations of the  $1.0 \text{ cm}^{-1}$  finite bin equivalent width for a line centered  $0.2 \text{ cm}^{-1}$  from the bin edge for a full range of atmospheric Lorentz and Doppler half-widths produces residuals in the single line transmittance no larger than 0.03, Figure 3 (left). The residuals are calculated by comparison to explicit numerical integration of the spectral transmittance from the Voigt line. When the MODTRAN4 algorithm is used to calculate the  $0.1 \text{ cm}^{-1}$  finite bin equivalent width for a line centered on the edge of the spectral bin, single line transmittance residuals increase above 0.20, Figure 3 (right). By including higher-order terms in the calculations of the line tail absorption, SERTRAN lowers the transmittance residuals for the  $1.0 \text{ cm}^{-1}$  equivalent widths to below 0.01, Figure 3 (left), and for the  $0.1 \text{ cm}^{-1}$  equivalent widths to below 0.03, Figure 3 (right). Thus, the accuracy (0.03) of the SERTRAN line center spectral transmittances at the SERTRAN bandwidth ( $0.1 \text{ cm}^{-1}$ ) is the same as the accuracy (0.03) of the MODTRAN4 line center spectral transmittances at the MODTRAN4 bandwidth ( $1.0 \text{ cm}^{-1}$ ).

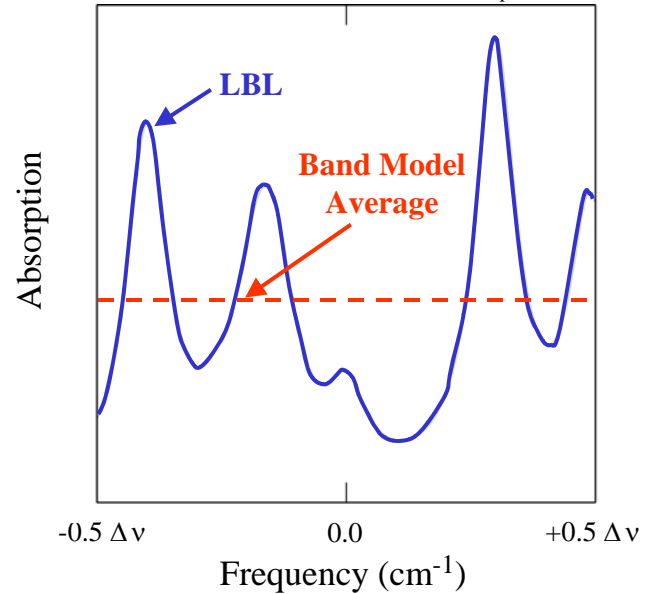


Figure 2: Comparison of Band Model and Line-By-Line Approaches. LBL models calculate high spectral resolution absorption (solid curve). Band models statistically determine the average integrated strength (dash line) based on line strength, line density, and line width parameters.

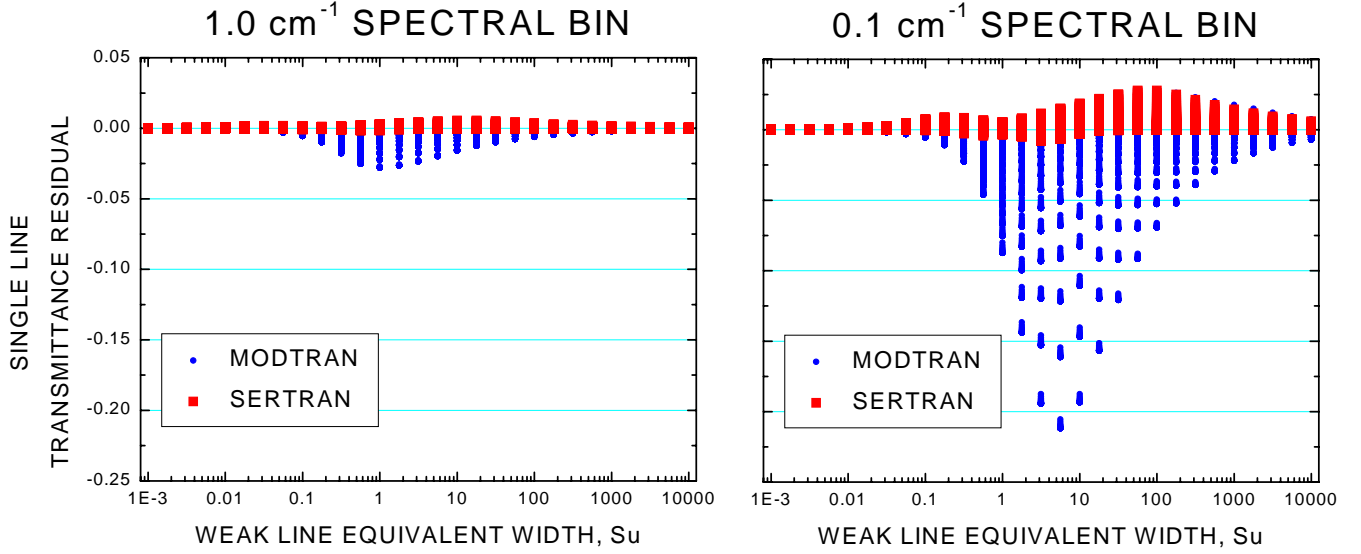


Figure 3: Residuals in  $1.0 \text{ cm}^{-1}$  (left) and  $0.1 \text{ cm}^{-1}$  (right) Single Line Transmittances for a Full Range of Lorentz and Doppler Half-Widths. The MODTRAN algorithm (small circle) is considerably less accurate than the SERTRAN algorithm (large squares).

## 2.2 SERTRAN band model line tail absorption

MODTRAN4  $1.0 \text{ cm}^{-1}$  band model line tail absorption is defined as the absorption from molecular transitions centered outside of the  $1.0 \text{ cm}^{-1}$  band but no more than  $25.5 \text{ cm}^{-1}$  from band center. Contributions from beyond  $25.5 \text{ cm}^{-1}$  are only considered for  $\text{H}_2\text{O}$  and  $\text{CO}_2$ , and modeled as continua. The line tail absorption is calculated from a database of temperature dependent  $0.25 \text{ cm}^{-1}$  integrated Lorentzian absorption coefficients. The line tail spectral dependence is assumed to be relatively flat so that the absorption coefficients can be modeled as constant on the  $0.25 \text{ cm}^{-1}$  spectral grid. To justify this assumption and enable line tails to be modeled as Lorentzian, molecular transitions centered too close to a  $1.0 \text{ cm}^{-1}$  spectral band edge are translated inward. A small line-shift correction is applied in-band to preserve the total integrated line strength. The overall error introduced into the  $1.0 \text{ cm}^{-1}$  band model by shifting line centers is small. In fact, early versions of the MODTRAN band model centered all lines located within a spectral band.

For SERTRAN, with its  $\Delta\nu = 0.1 \text{ cm}^{-1}$  band model, the MODTRAN4 line tail algorithm is inappropriate. Line tail spectral absorption cannot be modeled as constant or Lorentzian so close to line center. Also, as described in Section 2.1, the SERTRAN partition of line center and line tail contributions differs from the more traditional MODTRAN4 definition. Since the SERTRAN line center absorption includes contributions from molecular transitions centered as much as half a spectral bandwidth outside of the central spectral band, the line tail contribution is defined as the absorption from those lines centered more than half a bandwidth ( $0.05 \text{ cm}^{-1}$ ) from the central band. A major advantage of this new partitioning of the molecular absorption is that transition frequencies do not have to be shifted towards the center of a band to avoid the line centers being too close to an edge.

In SERTRAN, the use of a temperature-dependent *spectrally integrated* Lorentzian absorption coefficient database is replaced by a database of temperature and pressure dependent Padé approximant *spectral fits* to Voigt absorption coefficient curves. Five parameters,  $k_0, k_1, k_2, x_1$  and  $x_2$ , are used in the Padé fits:

$$\frac{k(\delta_\nu)}{P} = \frac{k_0 + k_1 \delta_\nu + k_2 \delta_\nu^2}{1 + x_1 \delta_\nu + x_2 \delta_\nu^2} ; \quad \delta_\nu = \frac{\nu - \nu_{cen}}{\Delta\nu/2} \quad (2)$$

In this parameterization,  $\nu_{cen}$  is the central frequency of the spectral band and the range of the normalized spectral variable  $\delta_\nu$  is from -1 to +1. Since the Lorentz line shape is proportional to pressure to leading order, the absorption coefficient over pressure  $P$  is fit to the Padé approximant. This form for the tail contributions yields an exact spectral fit in the limit of a single Lorentz tail. The five Padé parameters are determined from the summed line tail spectral absorption coefficients at the

center and edges of the spectral band, the spectral frequency derivative of the absorption coefficient at  $\nu_{cen}$ , and the integral of the spectral absorption coefficient over the spectral band.

Generally, the Padé spectral fits are extremely accurate. An example is shown in Figure 4. In this case, hundreds of molecular transitions contribute to the 305K and 1 atm pressure H<sub>2</sub>O line tail absorption coefficient spectrum between 200.0 and 200.1 cm<sup>-1</sup>, the thick dashed curve. The 6 largest contributors to the curve from lines centered above 200.15 cm<sup>-1</sup> are shown as lines with squares, and the 2 largest contributors from lines centered below 199.95 cm<sup>-1</sup> are shown as lines with diamonds (note the break and change of scale in the ordinate axis). As described above, the Padé fit fixes the spectral curve values at 200.00, 200.05, and 200.10 cm<sup>-1</sup>, the spectral derivative at 200.05 cm<sup>-1</sup>, and the integrated value. In this case, as with most, the spectral fit lies directly on top of the high-resolution spectrum.

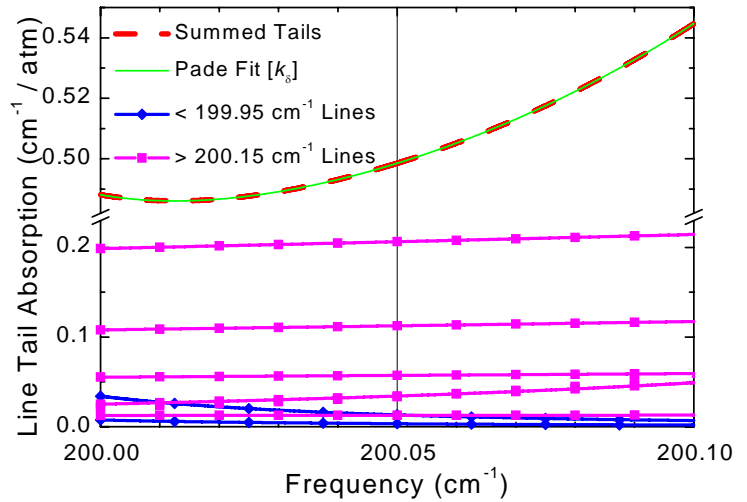


Figure 4: High Spectral Resolution Line Tail Absorption Curve (thick dash) and Padé Approximant Fit (thin line) for Lorentzian H<sub>2</sub>O Lines at 305K and 1 atm Pressure. The spectral curves from largest contributors are also illustrated (lines with diamond for lower frequency transitions and lines with squares for higher frequency transitions).

The spectral fit to the line tails is least accurate but still quite acceptable when the Doppler contribution is strong. The Padé form is unable to completely mimic the exponential decay of the Doppler line shape. For SERTRAN molecular bands, the worse fits result from near-IR O<sub>2</sub> lines and near-IR and visible H<sub>2</sub>O lines. In the example of Figure 5, the Doppler half-widths for the contributing H<sub>2</sub>O lines are near 0.019 cm<sup>-1</sup> and the atmospheric pressure is 0.1 atm. Although the Padé fit satisfies the 5 prescribed conditions, small but apparent residuals result.

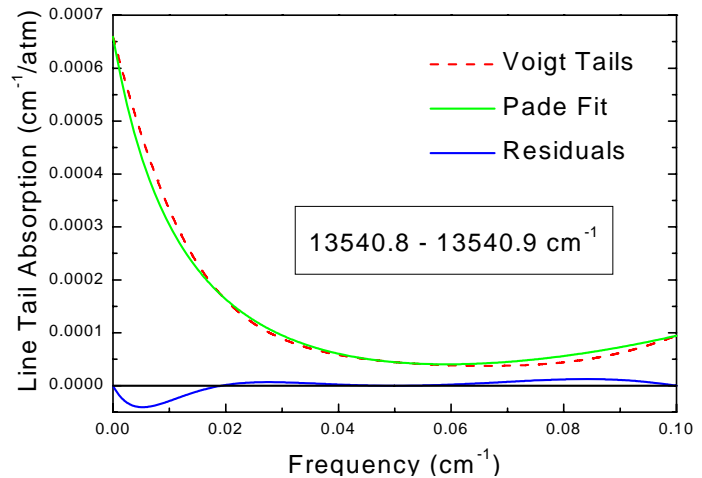


Figure 5: High Spectral Resolution Line Tail Absorption Curve (dash) and Padé Approximant Fit (solid) for Voigt lines with Strong Doppler Influence. The lower curve is the residual between the upper curves.

### 3. SERTRAN VALIDATION

SERTRAN validation efforts have concentrated on the LWIR through SWIR spectral regions. SERTRAN was validated by comparison to predictions of the FASE LBL model and to measurements from the High-resolution Interferometer Sounder (HIS) Fourier Transform Spectrometer<sup>13</sup>. The FASE model has itself been extensively validated against measured data, and it provides the benchmark for determining the accuracy of the SERTRAN band model results. The HIS spectrometer measures high quality, sub-wavenumber calibrated spectral radiances between 600 and 2700 cm<sup>-1</sup> (3.7 to 16.7 μm) for direct validation.

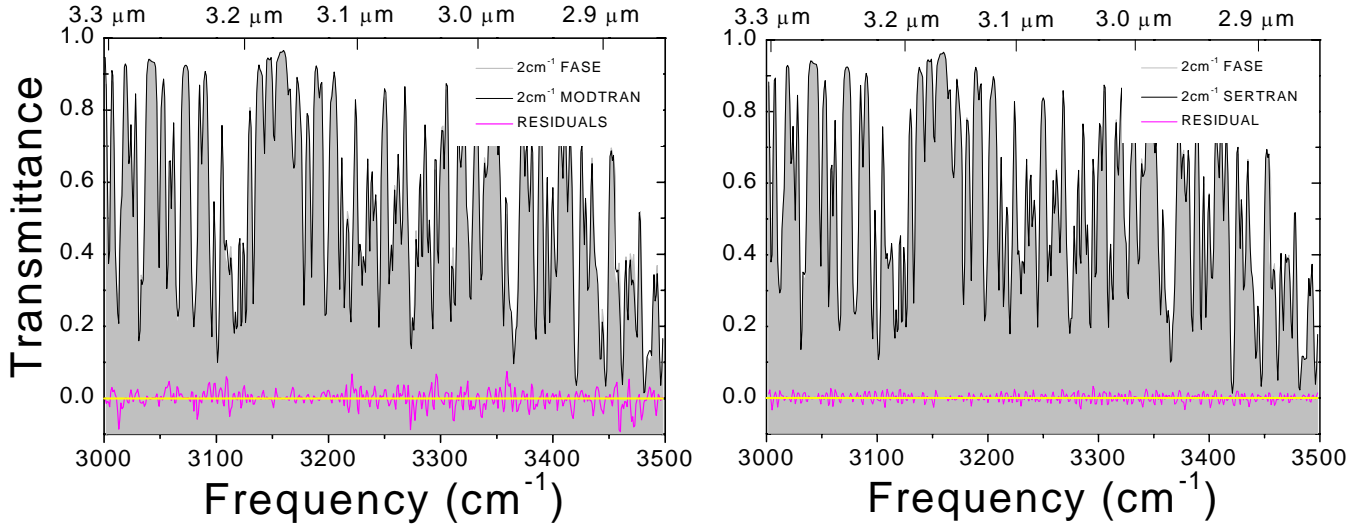


Figure 6: Validation Results for MODTRAN (left) and SERTRAN (right). The band model spectral transmittances are compared to FASE LBL predictions for a 0.5-km path at the ground. All three model results were convolved with the same  $2\text{ cm}^{-1}$  spectral response function.

### 3.1 SERTRAN to FASE validations

SERTRAN and FASE spectral transmittance predictions were compared for frequencies between  $500$  and  $4000\text{ cm}^{-1}$  ( $2.5$  to  $20\text{ }\mu\text{m}$ ) and for horizontal (constant pressure) paths between  $0$  and  $40\text{ km}$  altitude. Path lengths were selected to produce band average transmittances near  $50\%$  because transmittance residuals tend to be largest for transmittances near  $0.5$ .

The accuracy of individual band equivalent widths from  $0.1\text{ cm}^{-1}$  SERTRAN and  $1.0\text{ cm}^{-1}$  MODTRAN is comparable (Section 2.1). However, SERTRAN models line correlation and overlap more accurately because of its higher spectral resolution. Also, the SERTRAN line tail algorithm improves upon the MODTRAN algorithm. Thus, the SERTRAN to FASE residuals will be smaller than MODTRAN to FASE residuals when all three calculations are degraded to a common spectral resolution. This is illustrated in Figure 6. Spectral transmittances are compared for the  $0.5\text{ km}$  horizontal path at  $1\text{ atm}$  pressure containing U.S. Standard profile  $\text{H}_2\text{O}$ ,  $\text{CO}_2$ , and  $\text{O}_3$  concentrations. High spectral resolution SERTRAN and FASE predictions were convolved with a non-overlapping  $1\text{ cm}^{-1}$  rectangular slit, and subsequently degraded using a  $2\text{ cm}^{-1}$  triangular slit to mimic the MODTRAN  $2\text{ cm}^{-1}$  result. For both MODTRAN and SERTRAN, no strong bias is observed, i.e., the residual curves straddle the zero residual line. However, sporadic MODTRAN residuals approach  $0.1$  while all the  $2\text{ cm}^{-1}$  SERTRAN residuals are under  $0.02$ .

SERTRAN is compared to FASE at  $0.2\text{ cm}^{-1}$  spectral resolution in Figure 7. The scenario is identical to that of Figure 6, a  $1/2\text{-km}$  ground path with  $\text{H}_2\text{O}$ ,  $\text{CO}_2$ , and  $\text{O}_3$ . The spectral range has been reduced so that spectral details can be resolved. For much of the spectrum the residuals are under  $0.01$ , but occasional spikes are large as  $0.07$  are evident, consistent with the accuracy of the equivalent width residuals calculations.

Basic to the SERTRAN band model is the premise that molecular line absorption is substantial within two  $0.1\text{ cm}^{-1}$  spectral bins. At higher altitudes, this assumption breaks down - molecular line widths are small compared to the  $0.1\text{ cm}^{-1}$  bandwidth and most of the individual line absorption occurs in a single bin. As a result, SERTRAN essentially becomes a  $0.2\text{ cm}^{-1}$  band model. This is illustrated in Figure 8. SERTRAN  $0.2$

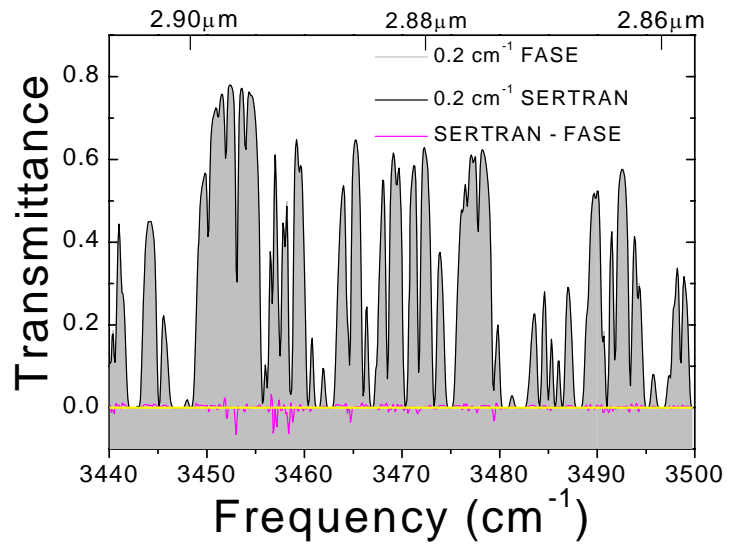


Figure 7: Comparison of FASE and SERTRAN  $0.2\text{ cm}^{-1}$  Spectral Transmittances near  $2.88\text{ }\mu\text{m}$ .

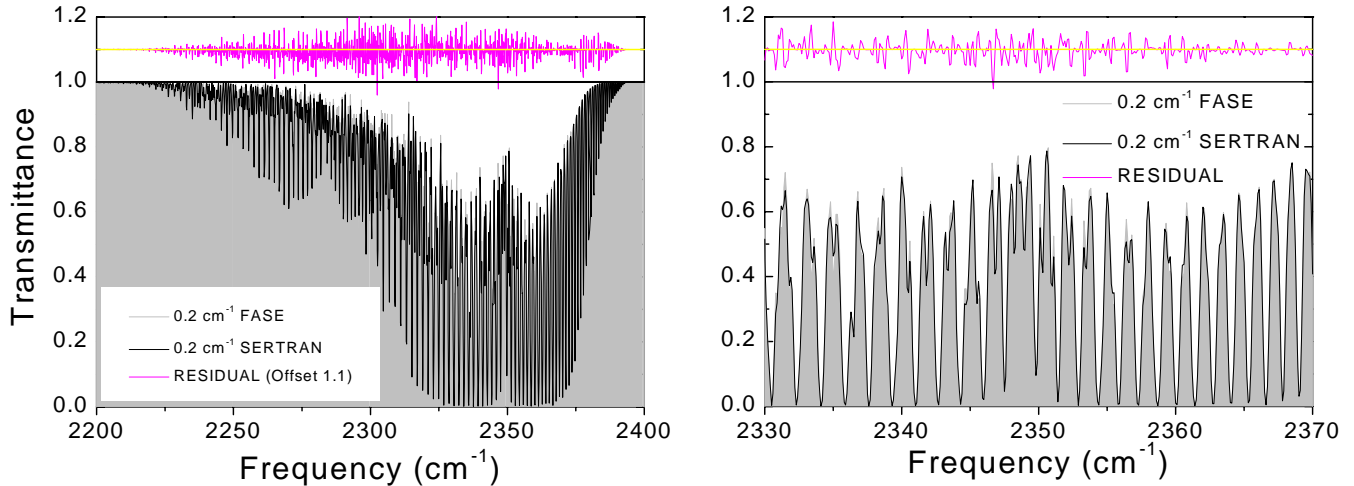


Figure 8: FASE and SERTRAN  $0.2 \text{ cm}^{-1}$  Spectral Transmittances for  $\text{CO}_2$  at 40-km Altitude and a 100-km Constant Pressure Path. The results are illustrated for the entire  $4.3\text{-}\mu\text{m}$  band (left) and an enlargement for the center of the band (right).

$\text{cm}^{-1}$  spectral transmittances are compared to FASE results for a horizontal path at 40-km altitude and with a 100-km range. The residuals are larger than at lower altitudes. Individual narrow yet strong absorption lines are equally partitioned into two  $0.1 \text{ cm}^{-1}$  spectral bins yielding too much absorption in one bin and too little in its neighbor.

### 3.2 SERTRAN to HIS validations

SERTRAN predictions were compared to HIS spectrometer measurements<sup>13</sup> from two separate campaigns: an airborne nadir measurement from 20-km altitude over the Pacific Ocean (14 April 1986) and a ground-based zenith measurement from the GAPEX experiment in Denver (31 October 1988). For both campaigns, atmospheric temperature and  $\text{H}_2\text{O}$  profiles were derived from radiosonde data. The validation results from the two sets of comparisons are similar. This paper presents the results from the nadir measurement comparison, for which a FASE validation was previously performed<sup>14</sup>.

HIS measurements for the  $600\text{-}1080 \text{ cm}^{-1}$  spectral band and the SERTRAN and FASE predictions are illustrated in Figure 9. The upper curves overlay the measured and modeled spectral radiances; the lower curves contain the *measurement minus model* residuals plotted with matched vertical scales. The HIS minus SERTRAN residuals are at the few percent level with spectral radiances and residuals near  $80$  and  $3 \text{ mW m}^{-2} \text{ sr}^{-1} / \text{cm}^{-1}$ , respectively. The unapodized HIS Fourier

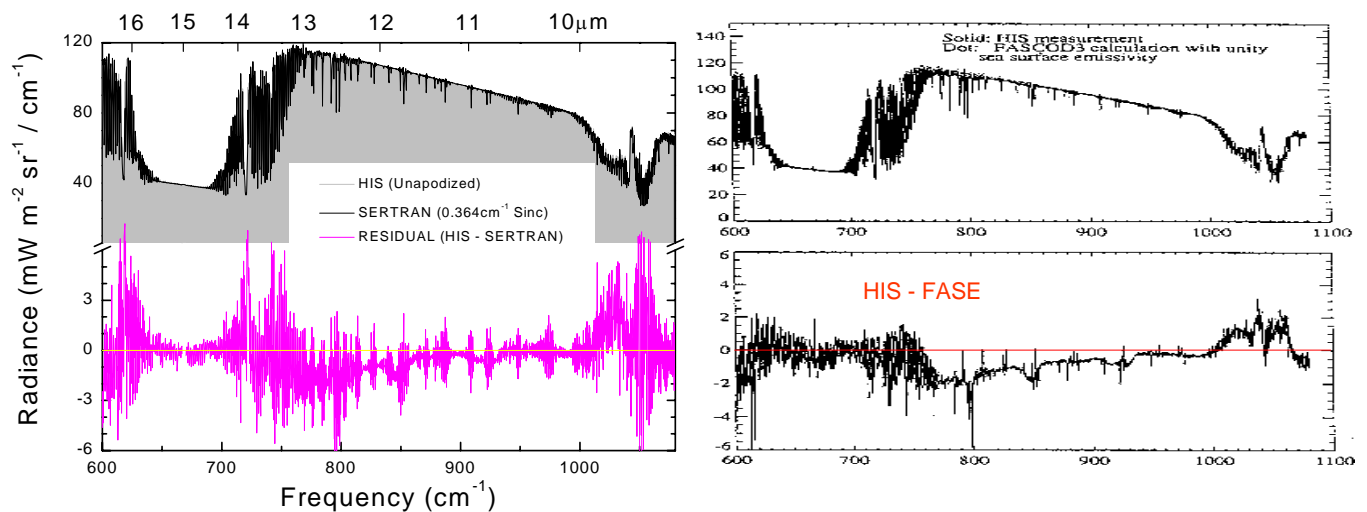


Figure 9: LWIR Validation of SERTRAN (left) and FASE (right) Spectral Radiances Against HIS Spectrometer Measurements for Nadir Viewing from 20-km Altitude over the Pacific Ocean (14 April 1986). SERTRAN radiances were convolved assuming a  $0.364 \text{ cm}^{-1}$  (FWHM) Sinc function.

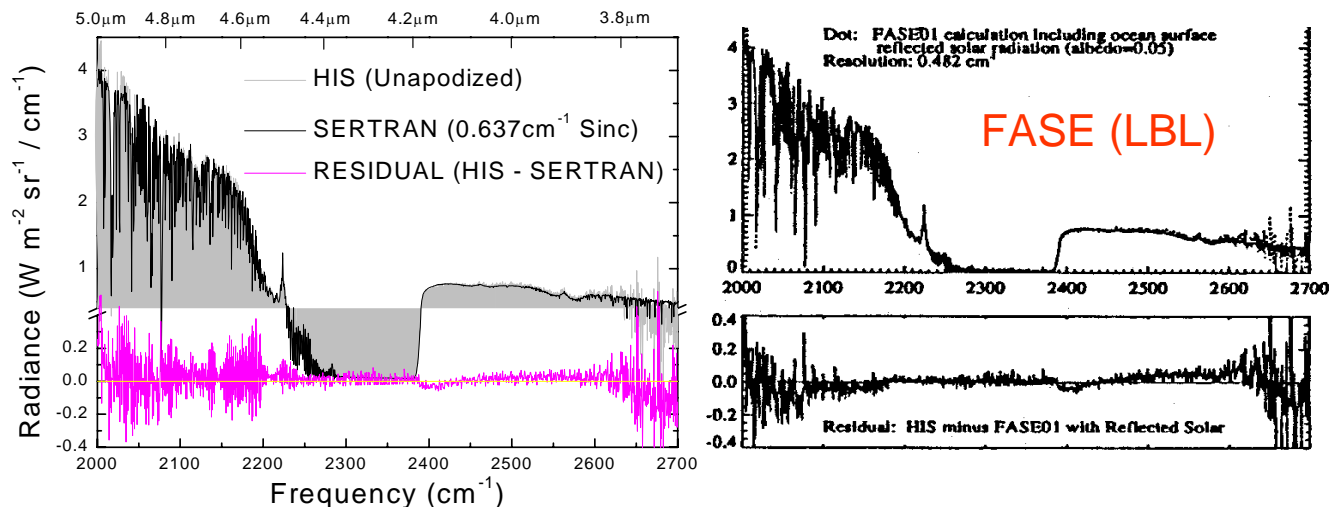


Figure 10: SWIR Validation of SERTRAN (left) and FASE (right) Spectral Radiances Against HIS Spectrometer Measurements for Nadir Viewing from 20-km Altitude over the Pacific Ocean (14 April 1986).

transform spectra were reported to have 0.364 cm<sup>-1</sup> spectral resolution in this band. For these comparisons, the SERTRAN results were computed using a 0.364 cm<sup>-1</sup> full width at half maximum (FWHM) sinc function. The results seem to indicate a mismatch in the filter function - the residuals contain more jitter than the earlier SERTRAN to FASE comparisons would suggest. Nevertheless, the agreement is good. Both SERTRAN and FASE modeled the sea surface as a blackbody (unit emissivity) which accounts for the baseline offset between 800 and 1000 cm<sup>-1</sup>. The residual spectrum between 1000 and 1080 cm<sup>-1</sup> indicates that the O<sub>3</sub> column amount was overestimated in the models - the main effect of the ozone is to attenuate the surface signal, and lowering the column amount should eliminate the 9.6 μm O<sub>3</sub> band spectral feature.

In the short-wave IR, the HIS spectrometer has a band extending from 2000 to 2700 cm<sup>-1</sup>, 3.7 to 5.0 μm, with a reported spectral resolution of 0.637 cm<sup>-1</sup>. Below around 4.0 μm, the solar components become important for daytime measurements. FASE includes the solar reflection off the surface in its nadir atmospheric radiance calculations (ocean surface albedo set to 5% in the SWIR model calculations), but atmosphere scattered solar radiance contributions are neglected. SERTRAN, like MODTRAN, includes the atmospheric scattered contributions in its calculations. This is evident in the SWIR HIS comparison, Figure 10. Between 2400 and 2600 cm<sup>-1</sup> FASE slightly under-predicts the spectral radiance. Although the SERTRAN predictions are noisier, the small bias in this region is decreased. This result had previously been demonstrated using MODTRAN, albeit with the spectral data degraded to 2 cm<sup>-1</sup>. The SERTRAN comparison has more jitter than the FASE comparison, especially between 2000 and 2200 cm<sup>-1</sup>, but again this is most likely due to a spectral filter mismatch. Otherwise, the SERTRAN and FASE results are comparable.

#### 4. CONCLUSIONS AND FUTURE DIRECTIONS

The reformulation of the MODTRAN band model and development of SERTRAN together provide a basis for future, rapid sub-wavenumber radiative transport analysis in the terrestrial atmosphere. The low-altitude IR validations performed to date demonstrate that SERTRAN achieves MODTRAN accuracy but at higher spectral resolution, with band *average* transmittance residuals of order 0.01 or better. Furthermore, comparisons of SERTRAN to MODTRAN at a common spectral resolution ( $\geq 2$  cm<sup>-1</sup>) show approximately a 4-fold decrease in residuals.

Even though the initial results are promising, for many applications such as retrieval of surface temperatures and spectral emissivity, greater model accuracy and additional validation is required to drive residuals down to measurement accuracy. Improved accuracy can be achieved without significant increases in computation time by refining the SERTRAN band model. Some specific tasks include (1) improving and optimizing equivalent width calculations, (2) tuning the band model based on high spectral resolution, pressure dependent line overlap calculations, and (3) incorporating the effects of self-broadening and line coupling.

## ACKNOWLEDGEMENTS

The authors wish to acknowledge the technical support of Paul Lewis CMO / SITAC (Central MASINT Office / Spectral Information Technology Applications Center). The HIS data was kindly supplied by the Cooperative Institute for Meteorological Satellite Studies (CIMSS) at the University of Wisconsin-Madison, courtesy of H.E. Revercomb. The original calculations were done in cooperation with H.E. Snell (Atmospheric and Environmental Research, Inc.) and J. Wang (National Center for Atmospheric Research).

## REFERENCES

1. A. Berk, G.P. Anderson, P.K. Acharya, L.S. Bernstein, J.H. Chetwynd, M.W. Matthew, E.P. Shettle and S.M. Adler-Golden, "MODTRAN4 User's Manual," Air Force Research Laboratory Report, June 1999.
2. A. Berk, L.S. Bernstein, G.P. Anderson, P.K. Acharya, D.C. Robertson, J.H. Chetwynd and S.M. Adler-Golden, "MODTRAN Cloud and Multiple Scattering Upgrades with Application to AVIRIS," *Remote Sens. Environ.* **65**, pp. 367-375, 1998.
3. S.A. Clough, F.X. Kneizys, G.P. Anderson, E.P. Shettle, J.H. Chetwynd, L.W. Abreu, and L.A. Hall, "FASCOD3 Spectral Simulation," *Proceedings of the International Radiation Symposium*, Lenoble and Geleyn, Deepak Publishing, 1988.
4. H.E. Snell, J.-L. Moncet, G.P. Anderson, J.H. Chetwynd, S. Miller, and J. Wang, "FASCOD for the Environment (FASE)," *Proceedings of Atmospheric Propagation and Remote Sensing IV, SPIE*, **2471**, pp. 88-95, 1995.
5. L.S. Bernstein, A. Berk, D.C. Robertson, P.K. Acharya, G.P. Anderson, and J.H. Chetwynd, "Addition of a Correlated- $k$  Capability to MODTRAN," *Proceedings of the 1996 Meeting of the IRIS Specialty Group on Targets, Backgrounds, and Discrimination*, Vol. III, pp. 249-258, 1996.
6. A.R. Curtis, Contribution to a Discussion of "A Statistical Model for Water Vapor Absorption," by R. M. Goody, *Quart. J. Roy. Meteorol. Soc.* **78**, pp. 638-640, 1952.
7. W.L. Godson, "The Evaluation of Infrared-Radiative Fluxes Due to Atmospheric Water Vapor," *Quart. J. Roy. Meteorol. Soc.* **79**, pp. 367-379, 1953.
8. R.G. Isaacs, W.C. Wang, R.D. Worsham and S. Goldenberg, "Multiple Scattering LOWTRAN and FASCOD Models," *Applied Optics* **26**, pp. 1272-1281, 1987.
9. K. Stamnes, S.C. Tsay, W.J. Wiscombe and K. Jayaweera, "Numerically Stable Algorithm for Discrete-Ordinate-Method Radiative Transfer in Multiple Scattering and Emitting Layered Media", *Applied Optics*, **27**, pp. 2502-2509, 1988.
10. L.S. Rothman, C.P. Rinsland, A. Goldman, S.T. Massie, D.P. Edwards, J.-M. Flaud, A. Perrin, V. Dana, J.-Y. Mandin, J. Schroeder, A. McCann, R.R. Gamache, R.B. Wattson, K. Yoshino, K. Chance, K.W. Jucks, L.R. Brown, V. Nemtchinov, and P. Varanasi, The HITRAN Molecular Spectroscopic Database and HAWKS (HITRAN Atmospheric Workstation): 1996 Edition, *J. Quant. Spectrosc. Radiat. Transfer*, **60**, pp. 665-710 (1998).
11. C.D. Rodgers and A.P. Williams, Integrated absorption of a spectral line with the Voigt profile, *J. Quant. Spectrosc. Radiat. Transfer*, **14**, pp. 319-323, 1974.
12. G.N. Plass, Models for Spectral Band Absorption, *J. Opt. Soc. Am.*, **48**, pp. 690-703, 1958.
13. H.E. Revercomb, H. Bujis, H.B. Howell, R.O. Knuteson, D.D. LaPorte, W.L. Smith, L.A. Sromovsky, and H.W. Woolf, "Radiometric calibration of IR interferometers: Experience from the High-Resolution Interferometer Sounder (HIS) aircraft instrument," RSRM '87, *Advances in Remote Sensing Retrieval Methods*. A. Deepak, H. Fleming, and J. Theon, Eds. 1989.
14. J. Wang, G.P. Anderson, H.E. Revercomb, and R.O. Knuteson, "Validation of FASCOD3 and MODTRAN3: Comparison of Model Calculations with Ground-Based and Airborne Interferometer Observations Under Clear-Sky Conditions," *Appl. Optics*, **35**, pp. 6028-6040, 1996.